Bio-Medical Materials and Engineering 14 (2004) 13–22
IOS Press 

# Comparison of mechanical properties of rat tibialis anterior tendon evaluated using two different approaches

John Z. Wu *, Anne Brumfield, Gerald R. Miller, Rebecca Metheny and Robert G. Cutlip
*National Institute for Occupational Safety and Health, Morgantown, WV, USA*

Received 3 February 2003

**Abstract.** Tendon injuries may result in variations of its mechanical properties. The published data of the tendon stiffness of small animals, such as mouse and rat, are exclusively obtained by measuring grip-to-grip (g-t-g) displacement. Local strain concentration and relative sliding of the specimens in the clamps might significantly affect the measured tendon deformation. In the present study, the mechanical properties of the rat tibialis anterior tendon measured using the proposed tendon mark method were compared to those evaluated using the g-t-g displacement method. Five male Sprague Dawley rats (~418 g) were used in this study. For the proposed method, reference marks were made on the tendons using permanent ink. A microscope video system was customized to observe and record the tendon deformation. Pattern recognition software was developed to obtain the displacement time-histories of the reference marks. The distance between the grips was approximately 7 mm; and the distance between the reference marks used for the data processing was approximately 5 mm. The cross-section areas of the specimens were measured using a custom-made slot gauge and by applying a constant compressive stress (0.15 MPa). The tendons were clamped between two custom-made metal grips and stretched on a testing machine at a constant speed (1 mm/s) up to failure. Throughout the tests, the tendon specimens were submerged in a PBS bath at 22°C. The deformation of the specimens was evaluated using the g-t-g displacement method and the proposed method. The stress/strain curves obtained by using the g-t-g displacement can be characterized by an initial toe zone, a quasi-linear zone, and a final failure stage. The stress/strain curves determined using the proposed method are quite different from those obtained using the g-t-g displacement: it has a smaller toe zone and a stress-hardening transition, over which the tendon stiffness increases dramatically with the increasing strain. The tendon stiffness measured by using the g-t-g displacement method may underestimate the actual mechanical properties of tendon by approximately 43%.

## 1. Introduction

Tendons are skeletal connective tissue that performs important mechanical functions. Tendons transmit forces from muscles to bones and experience much higher stress during locomotion than any other component in the musculoskeletal system. Under prolonged or repetitive loading, tendons frequently suffer from injuries [1–3]. From a structural point of view, tendons are collagenous tissues, composed mainly of extracellular matrix (collagen fibers) and interstitial fluid (e.g., [4]). Mechanical loading may induce the initiation and development of damage in tendons' extracellular matrix. The accumulation of damage in the tendon tends to degrade the tendon's mechanical properties, and finally, leads to failure. As the variations in the mechanical properties may provide essential information for the evaluation of tendon injuries and the causal mechanisms, the mechanical characteristics of mammalian tendons have been studied by many researchers (e.g., [5–7]).

*Corresponding author: John Z. Wu, PhD, NIOSH, 1095 Willowdale Road, Morgantown, WV 26505, USA. Tel.: +1 304 285 5832; Fax: +1 304 385 6265; E-mail: jwu@cdc.gov.

Small animals, such as the mouse and rat, have been widely used for the study of the mechanical characteristics of tendons. Compared to large animals, the use of small animals has many advantages: small animals are relatively cheaper to raise and purchase, so that a greater number of animals can be used for testing at a lower cost, improving the reliability of the experimental results; the life cycle of small animals is relatively shorter, consequently, the test results can be achieved within a shorter time period. However, due to the dimensions of the specimens, it is technically more difficult to obtain reliable tendon mechanical characteristics using small animals. One of the technical difficulties for testing small animal tendons is to evaluate the tendon deformation. The published data of the tendon stiffness of small animals are exclusively obtained by measuring grip-to-grip (g-t-g) displacement (e.g., [7–10]). The tendon deformation measured using the g-t-g method may include errors of unknown magnitude. First, due to the local strain concentrations in the tendon specimen near the grip site, the tendons are usually not deformed uniaxially. Secondly, the sliding of the tendon specimen relative to the grips cannot be eliminated, even in optimal conditions. All these effects will confound the measured deformation of the tendon specimen using the g-t-g method; consequently, the tendon stiffness measured using such an approach may not reflect the true mechanical characteristics of the tendon.

The purposes of the present study are: (a) to develop an approach to evaluate the stress/strain characteristics of the tendons of small animals; (b) to evaluate the errors of the strains of small animal tendons using the traditional g-t-g method. Tibialis anterior tendons of Sprague Dawley rats are to be used in the present study. The tendons are to be stretched on a micro-mechanical testing machine at a constant speed up to failure. The deformation of the specimens is to be evaluated using the displacements between the grips (g-t-g method) and between the reference marks using the proposed optical method. The stress/strain curves obtained using these two methods will be evaluated and compared.

## 2. Method

### 2.1. Sample preparation

Five male Sprague Dawley rats (418 $\pm$ 13 g, 12 weeks of age) were used in the study. All animals were housed in the animal quarters associated with the laboratory. Temperature and light/dark cycle were held constant for all animals; food and water were provided *ad libitum*. All animals were subjected to a standardized experimental protocol approved by the Animal Care and Use Committee of NIOSH before conducting the experimental protocols.

Five rats were sacrificed in the present study. The tibialis anterior tendons of the right and left hind limbs of each animal were isolated. The preparations of four tendons were not successful, so that six tendons were available for the study.

After being dissected from the rats, the tendons were sealed in plastic bags and kept in a freezer at $-80^{\circ}$C. Before the tests, the tendons were defrosted in PBS solution bath at room temperature (22°C) for at least three hours. The effects of freezing preservation on the elastic and viscoelastic properties of tendons have been found to be negligible (e.g., [11,12]).

### 2.2. Experimental set-up

The experimental set-up for the tendon tests is illustrated in Fig. 1. Each tendon specimen was clamped between two custom-metal grips. The grip complex was composed of fixed blocks and sliding grips. The grips slide in the v-shaped slots of the fixed blocks during pulling, such that the gripping force increased

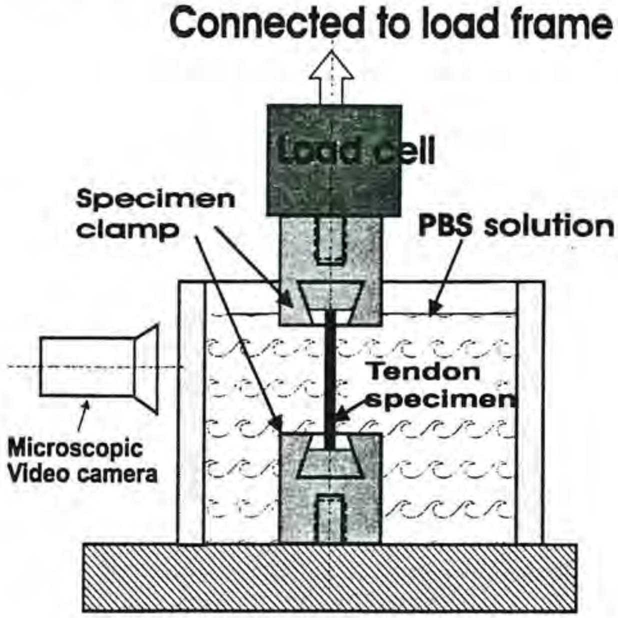


Fig. 1. Schematics of the set-up for tendon tests. The tendon specimen was clamped between two self-tightening grips. The deformation of the tendon was measured using a microscopic video system as well as from the relative displacement between the grips. The tendon specimens were submerged in phosphate-buffered saline (PBS) solution at room temperature (22°C) throughout the tests.

with increasing stretch force. In order to increase the friction force between the tendon and grips, the contact surface of the grips were covered with fine sand paper (grit # 200). The tests were performed using a universal micro-mechanical testing machine (type Mach-I, Biosyntech, Montreal, Canada). The testing machine was equipped with a displacement sensor with a resolution of 0.5 $\mu$m and a 98 N (10 kg) load cell with a resolution of 4.50 mN (500 mg). Both tendon specimen and grips were submerged in PBS solution (Sigma Diagnostics, St. Louis, Missouri, USA).

Reference marks were made on the tendons using permanent ink before they were installed on the testing machine. Since the resolution of the position recognition of the tendon mark is limited, two marks with the maximal distance between them, i.e., the marks near the clamping sites, were used as the reference marks, such that the measurement errors could be minimized. The distance between the grips was approximately 7 mm. And the distance between the reference marks used for the data processing was approximately 5 mm. The deformation of the specimens was evaluated using the relative displacements between the grips and between the reference marks.

The microscope video system included a color CCD camera (JAI, Woburn, Massachusetts, USA) and a microscope video lens (Infinity Photo-Optical Company, Boulder, Colorado, USA). LabView IMAQ Vision software, a PCI-1422 Framegrabber, and an AI-16XE-50 DAQCard (National Instruments, Houston, TX, USA) were used to record the displacement of the tendon marks during loading. A customized user interface provided calibration, resolution validation, image capture, and image post-processing routines. One of the DAQCard counters was used to trigger the buffered image acquisition at a rate of 10 Hz. The timing and system capabilities were tested and verified using a rubber band prior to the tendon tests. Displacement time-histories of the reference marks were obtained using pattern recognition algorithms with region-of-interest subroutines to eliminate error due to false positive recognitions.

The cross-section areas of the specimens were measured using a custom-made slot gauge, as shown in Fig. 2. The stainless steel slot gauge had a width of 0.80 mm and a depth of 6.3 mm. The slot gauge was attached to a digital caliper with a resolution of 0.01 mm. A constant compressive stress (0.15 MPa) was

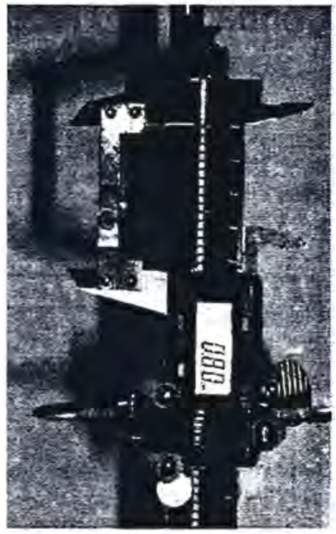

Fig. 2. Determination of the cross-sectional area of tendon using a digital slot-gauge. The tendon specimen was put into the slot and compressed via a weight to reach a compressive stress of 0.15 MPa. The cross-sectional area was read by a digital calliper.

applied on each tendon specimen via a dead weight (Fig. 2), such that the cross section of the tendon specimen was compressed to take the shape of the slot gauge. Similar techniques have been used for large animal tendons (e.g., [13]).

### 2.3. *Test procedure*

In order to obtain repeatable test results, each tendon specimen was preconditioned via sinusoidal, cyclic loading for 60 seconds, which was performed using a displacement protocol with a peak strain magnitude of approximately 0.05%. Each tendon was then relaxed for 30 seconds, and stretched up to failure at a loading speed of 1 mm/s. Throughout the tests, the tendon specimens were submerged in PBS (Sigma Diagnostics, St. Louis, Missouri, USA) solution at room temperature ($22 \pm 0.5$°C). The tendon stress was calculated by dividing the tendon force over the cross-sectional area at the unloaded state; the tendon strain was defined as the tendon deformation (i.e., the relative displacement between the grips or the reference marks) divided by the reference length (i.e., the distance between the grips or tendon reference marks at the undeformed state).

## 3. Results

Figure 3 shows the typical deformation pattern of the tendon during the stretch. The tendon strain was evaluated using the displacements of g-t-g and tendon marks, respectively. The tendon mark displacements were calculated using the displacements of two marks near the tendon grips. The positions of the reference marks during the stretch were determined by monitoring the edges of the marks via the pattern recognition system (Fig. 3). The strain value shown in Fig. 3 is the g-t-g strain, which serve as an indicator for the extent of the tendon stretch. It is seen from the figures that the length of the tendon is almost unchanged while the relative displacement between the grips is increased extensively, suggesting that the strain determined using the g-t-g displacement is mainly due to the relative sliding at the tendon gripping sites, not the real tendon deformation.

The stress/strain curves for six different tendon specimens obtained using two approaches are compared in Fig. 4. The stress/strain curves obtained using the g-t-g displacement (Fig. 5A) for all six tests

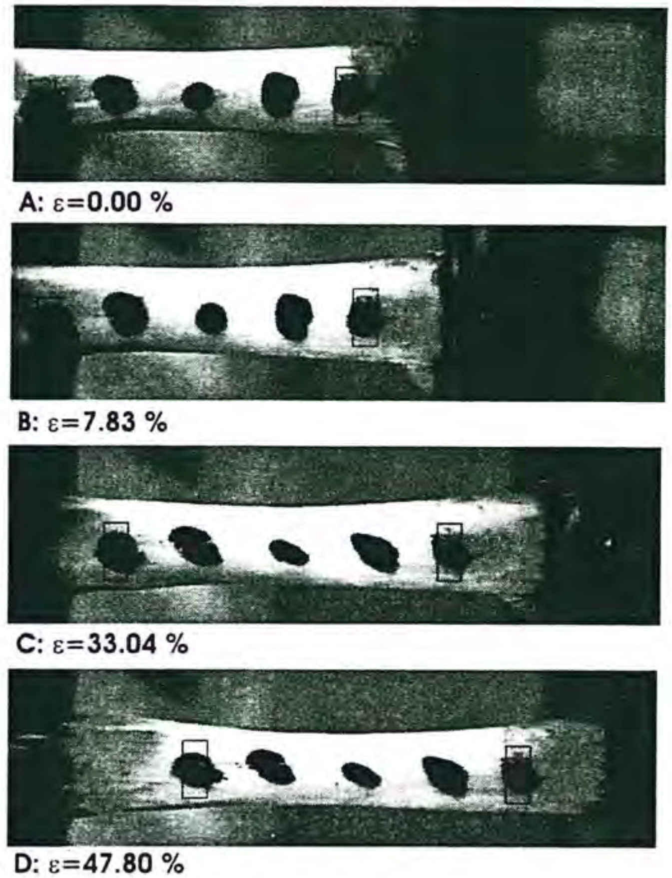


Fig. 3. Typical deformation patterns of the tendon during stretch. The tendon was stretched at a speed of 1.00 mm/s up to failure. A pattern recognition system was applied to recognize two predetermined marks near the clamping sites on the tendon, as shown in the pictures. The figures show that the tendon begins to fail at the position near clamping sites when the nominal elongation reaches approximately 47% (D). The actual tendon deformation, which is measured via the tendon marks, is much smaller then the nominal strain estimated via the g-t-g displacement. The strain values shown in figures are the nominal strain, which are estimated using the g-t-g displacement.

are plotted together and compared to those obtained using the tendon mark displacements (Fig. 5B). The stress/strain curves obtained by using the g-t-g displacement can be characterized by three stages (Fig. 5A), i.e., an initial toe zone, in which the stiffness increases relatively slowly with increasing deformation, a quasi-linear zone, in which the stress/strain relationship is approximately linear, and a final failure stage, at which the stress first reaches its maximum and then decreases with increasing strain. The stress/strain curves determined using the tendon marks are quite different from those obtained using the g-t-g displacement (Fig. 5B): it has a smaller toe zone and no obvious failure stage, but a stress-hardening transition (at a stress level of approximately 20 MPa), over which the tendon stiffness increases dramatically with increasing strain.

In the present study, the tangent tendon stiffness was used to evaluate the tendon mechanical characteristics. For the stress/strain curves obtained using the tendon marks, the stiffness was evaluated at a stress-hardening transition, the stress level when the stiffness begins to increase dramatically (Fig. 6). At the same stress level, the stiffness of the stress/strain curves obtained using the g-t-g displacement was obtained, as shown in Fig. 6.

The stress and strain at failure ($\sigma_f$ and $\varepsilon_f$, respectively), stress and strain at the stress-hardening transition ($\sigma_m$ and $\varepsilon_m$, respectively), and the stiffnesses estimated using the tendon marks and g-t-g displacement ($S_{\text{mark}}$ and $S_{\text{g-t-g}}$, respectively) for all six tests are summarized in Table 1. The average tendon

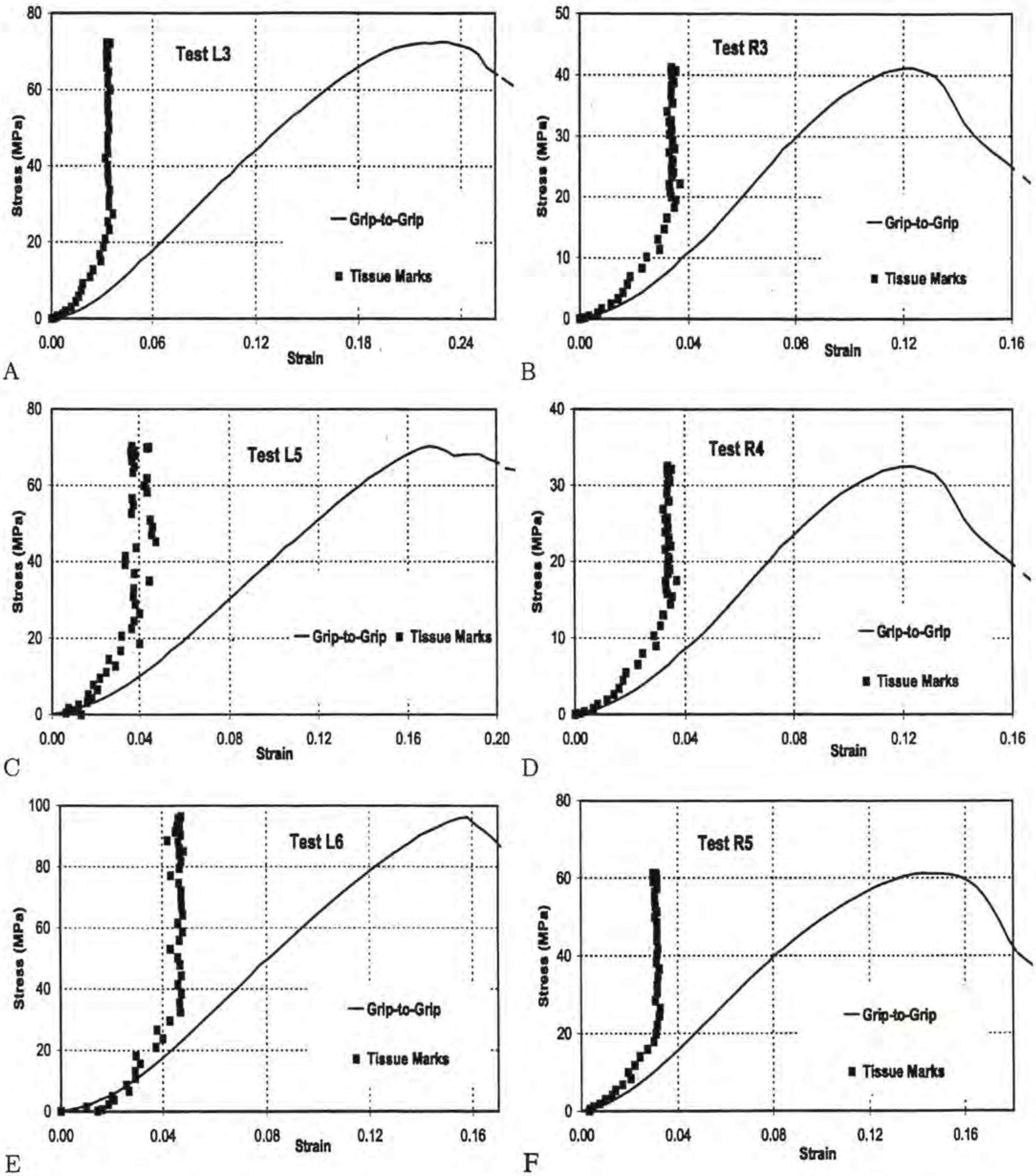


Fig. 4. Stress/strain curves of tendon during stretch obtained using the g-t-g and tendon mark displacements, respectively. The tendons were stretched at a speed of 1.00 mm/s. A, B, C, D, E, and F are the stress/strain curves obtained using six different tendon specimens. The stress/strain curves obtained using tendon mark displacements show different pattern than those obtained via g-t-g displacements.

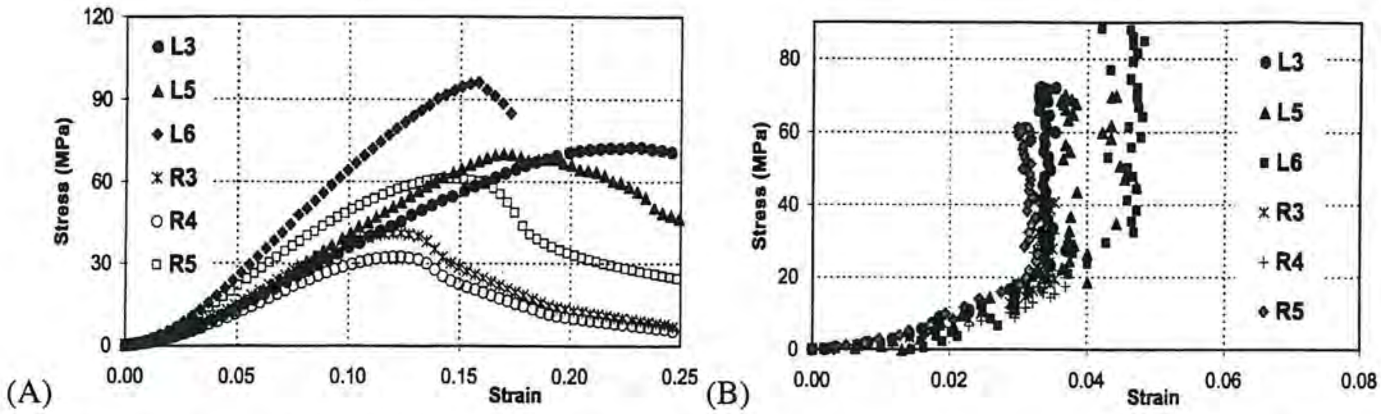


Fig. 5. Stress/strain curves of tendon during stretch obtained using the g-t-g (A) are compared to those obtained from the tendon mark displacements (B). These stress/strain curves are re-plotted using the data shown in Fig. 4.

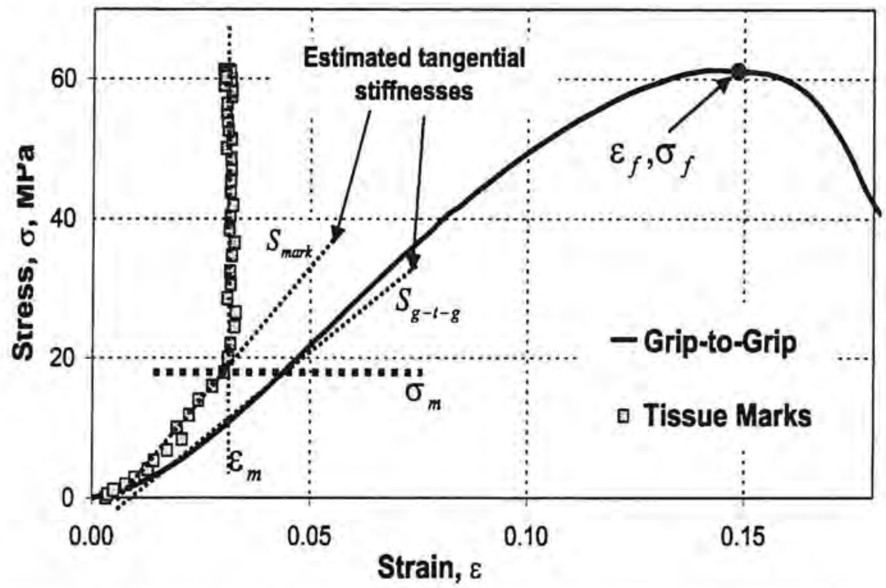


Fig. 6. Schematics of the test data process. The figure shows the methods to estimate the stress and strain at failure ($\sigma_f$ and $\varepsilon_f$, respectively), the stress and strain at the stress-hardening transition ($\sigma_m$ and $\varepsilon_m$, respectively), and the tendon tangent modulus or stiffness. The tangent stiffness evaluated using the approaches of the tendon marks and g-t-g displacement is defined as $S_{\text{mark}}$ and $S_{\text{g-t-g}}$, respectively.

stiffness obtained using the tendon marks is 806.2 ($S_\sigma = 88.3$) MPa; while that obtained using the g-t-g displacement is 461.9 ($S_\sigma = 73.3$) MPa. The average stress and the strain at the stress-hardening transition are 19.61 ($S_\sigma = 2.11$) MPa and 0.0366 ($S_\sigma = 0.0023$), respectively. The average stress and strain at failure are 62.36 ($S_\sigma = 9.41$) MPa and 0.158 ($S_\sigma = 0.016$), respectively.

## 4. Discussion and conclusion

Mechanical properties of tendons have been studied by many researchers for several decades. The approach to determine the tendon deformation during stretch directly affects the stress/strain curves of tendons. In most mechanical tests using small animal tendons (e.g., [2,7–10]), the deformations were estimated from the relative displacements between the specimen grips. Such a treatment may introduce unpredictable errors, due to the relative sliding between the tendon specimen and grips and the local

Table 1

Summary of tendon test results. The stress and strain at failure ($\sigma_f$ and $\varepsilon_f$, respectively), stress and strain at the stress-hardening transition ($\sigma_m$ and $\varepsilon_m$, respectively), and the stiffnesses estimated using the tendon marks and g-t-g displacement ($S_{\text{mark}}$ and $S_{\text{g-t-g}}$, respectively) for all six tests are listed

| Test No. | $\sigma_f$ (MPa) | $\varepsilon_f$ | $\sigma_m$ (MPa) | $\varepsilon_m$ | $S_{\text{g-t-g}}$ (MPa) | $S_{\text{mark}}$ (MPa) |
|---|---|---|---|---|---|---|
| L3 | 72.59 | 0.227 | 18.75 | 0.0344 | 382.8 | 754.1 |
| L5 | 70.27 | 0.169 | 18.63 | 0.0381 | 426.1 | 801.1 |
| L6 | 96.26 | 0.158 | 29.61 | 0.0471 | 784.8 | 1161.5 |
| R3 | 41.22 | 0.124 | 18.29 | 0.0346 | 426.4 | 869.9 |
| R4 | 32.54 | 0.123 | 14.43 | 0.0341 | 246.4 | 492.7 |
| R5 | 61.25 | 0.145 | 17.95 | 0.0313 | 505.1 | 757.6 |
| Mean | 62.36 | 0.158 | 19.61 | 0.0366 | 461.9 | 806.2 |
| Std. error ($S_\sigma$) | 9.41 | 0.016 | 2.11 | 0.0023 | 73.3 | 88.3 |

strain concentration in the tendon near the clamping sites. The effective reference specimen length cannot be well defined with such an approach. Wren et al. [14] found that the yield strain obtained from tendon marks was approximately 50% smaller than that from g-t-g displacement for human Achilles tendon. For short small animal tendons, such as the Achilles and tibialis anterior tendons of rats, the mechanical characteristics were exclusively evaluated relying on the displacement of g-t-g. In the present study, we compared the stress/strain curves of rat tibialis anterior tendon obtained using the displacements of g-t-g and reference marks on the tendon and found that the traditional g-t-g approach may underestimate the tendon stiffness by approximately 43% ($p < 0.00012$). Our results suggest that the g-t-g approach is not reliable and may introduce measurement errors of unknown magnitude. We developed a system for testing small animal tendons, which made it possible, for the first time, to determine the true mechanical properties of the short small animal tendon.

Typical stress/strain curves obtained using g-t-g displacement are characterized by a toe region with a low stiffness followed by a steeper increase in the stiffness, as shown in Fig. 4. However, there is no obvious toe region for the stress/strain curves obtained from the tendon marks optically. Since the tendon deformation determined using the tendon marks is believed to reflect the true tendon deformation, the toe region on the stress/strain curves obtained using the g-t-g displacement may be an artifact, which is associated with the initial conditions of the mechanical loading and clamping system. The true stress/strain relationship may not have the toe region, as traditionally described.

The mechanical properties of tendons have been traditionally characterized using the stress and strain at failure (e.g., [7,8]). Our results show that the measured tendon strain values at failure, which are obtained using the g-t-g displacement, are approximately four times greater than those at the stress-hardening transition, which are obtained using the tendon marks. This is because the measured tendon strain values at failure are attributed mostly by the relative sliding between the specimen and the grips. Therefore, the strains at failure are not representative of the real tendon deformations.

In the present study, the cross-sectional area of the tendon was measured using a slot gauge by applying a constant pressure of approximately 0.15 MPa. The cross-sectional area determined using such an approach was approximately 10% smaller than that determined using a non-contact optical method (e.g., laser scan, ultrasonic technique) [15–17]. However, for small animal tendons with a dimension of 0.1–0.5 mm, it is technically difficult to determine the cross-sectional area using the laser scan technique.

Thus, the slot gauge approach is the only reliable method, to the authors' best knowledge, for measuring the cross-sectional area of small tendon.

The mechanical properties of tendon might be temperature-dependent. In order to simulate the physiological environment, many reported tendon test data were obtained at a temperature of ~37°C (e.g., [13]). In the present study, however, the tendons were tested at a temperature of 22°C. Since the purpose of the present study is to compare the mechanical characteristics of the tendon obtained using two different approaches, the test temperature has no impact on the conclusions obtained in the study.

In the present study, the stress/strain curves of the tendon were obtained using a single loading rate (1.00 mm/s). Theoretically, the mechanical characteristics of tendon should be loading-rate-dependent due to the viscous properties of the material. Yamamoto and Hayashi [18] tested rabbit patellar tendon at a range of loading rates from 0.33 mm/s to 560 mm/s and found that the stress and strain at failure increased with increasing loading rate while the tangent modulus (stiffness) was independent of the loading rate. Wren et al. [14,19] found from their tests using human Achilles tendon that the loading rate had negligible effects on the tendon stiffness measurements, while influenced the failure stress. Since we are mainly interested in the tendon stiffness and the stress/strain relations before failure, the loading rate should have negligible impact on our results.

The limitation of the proposed approach for measuring the tendon deformation is that it cannot be used for large deformation shortly before the failure, since the tendon deforms so much that the ink marks on the tissue cannot be recognized by the pattern recognition system. One possible way to solve such a problem is to identify the tendon deformation manually from the recorded video in the large deformation range.

A comparison of these two approaches to measure the tendon stiffness shows that both methods could introduce measurement errors. In the case of the g-t-g displacement approach, the errors come from loading configurations, i.e., due to the specimen/grip sliding and strain concentration in the specimen, consequently, the experimental results cannot be repeated in different labs. In the case of the tendon mark approach, the errors are a result of the limitations of the system resolution and the accuracy of the pattern recognition program to dynamically define the tendon markings as the tendon undergoes deformation. Optimization of the system resolution, i.e., via preferred camera and lens selections, significantly reduces the magnitude of the error range. Using this method, experimental results should be reproducible in different laboratories.

## References


[1] H. Schechtman and D.L. Bader, In vitro fatigue of human tendons, *J. Biomech.* **30**(8) (1997), 829–835.

[2] C.I. Buchanan and R.L. Marsh, Effects of long-term exercise on the biomechanical properties of the achilles tendon of guinea fowl, *J. Appl. Physiol.* **90**(1) (2001), 164–171.

[3] H. Schechtman and D.L. Bader, Fatigue damage of human tendons, *J. Biomech.* **35**(3) (2002), 347–353.

[4] D.F. Betsch and E. Baer, Structure and mechanical properties of rat tail tendon, *Biorheology* **17**(1–2) (1980), 83–94.

[5] K. Kubo, H. Kanehisa, M. Ito and T. Fukunaga, Effects of isometric training on the elasticity of human tendon structures in vivo, *J. Appl. Physiol.* **91**(1) (2001), 26–32.

[6] C.N. Maganaris and J.P. Paul, In vivo human tendon mechanical properties, *J. Physiol.* **521** Pt 1 (1999), 307–313.

[7] T. Mullner, O. Kwasny, R. Reihsner, V. Lohnert and R. Schabus, Mechanical properties of a rat patellar tendon stress-shielded in situ, *Arch. Orthop. Trauma Surg.* **120**(1–2) (2000), 70–74.

[8] M.I. Almeida-Silveira, D. Lambertz, C. Perot and F. Goubel, Changes in stiffness induced by hindlimb suspension in rat achilles tendon, *Eur. J. Appl. Physiol.* **81**(3) (2000), 252–257.

[9] P.D. Inhofe, W.A. Grana, D. Egle, K.W. Min and J. Tomasek, The effects of anabolic steroids on rat tendon. An ultrastructural, biomechanical, and biochemical analysis, *Am. J. Sports Med.* **23**(2) (1995), 227–232.

[10] E.M. Kumar and P.L. Vijayammal, Effect of exposure of cigarette smoke on mechanical properties and thermal behaviour of rat skin and tendon, *Indian J. Exp. Biol.* **35**(7) (1997), 776–779.
[11] R.F. Ker, Dynamic tensile properties of the plantaris tendon of sheep (ovis aries), *J. Exp. Biol.* **93** (1981), 283–302.
[12] F.H. Silver, D.L. Christiansen, P.B. Snowhill and Y. Chen, Role of storage on changes in the mechanical properties of tendon and self-assembled collagen fibers, *Connect. Tiss. Res.* **41**(2) (2000), 155–164.
[13] E. Yamamoto, S. Tokura, N. Yamamoto and K. Hayashi, Mechanical properties of collagen fascicles from in situ frozen and stress-shielded rabbit patellar tendons, *Clin. Biomech. (Bristol, Avon)* **15**(4) (2000), 284–291.
[14] T.A. Wren, S.A. Yerby, G.S. Beaupre and D.R. Carter, Mechanical properties of the human achilles tendon, *Clin. Biomech. (Bristol, Avon)* **16**(3) (2001), 245–251.
[15] T.Q. Lee and S.L. Woo, A new method for determining cross-sectional shape and area of soft tissues, *J. Biomech. Eng.* **110**(2) (1988), 110–114.
[16] A. Race and A.A. Amis, Cross-sectional area measurement of soft tissue. A new casting method, *J. Biomech.* **29**(9) (1996), 1207–1212.
[17] C. Gillis, N. Sharkey, S.M. Stover, R.R. Pool, D.M. Meagher and N. Willits, Ultrasonography as a method to determine tendon cross-sectional area, *Am. J. Vet. Res.* **56**(10) (1995), 1270–1274.
[18] N. Yamamoto and K. Hayashi, Mechanical properties of rabbit patellar tendon at high strain rate, *Biomed. Mater. Eng.* **8**(2) (1998), 83–90.
[19] T.A. Wren, S.A. Yerby, G.S. Beaupre and D.R. Carter, Influence of bone mineral density, age, and strain rate on the failure mode of human achilles tendons, *Clin. Biomech. (Bristol, Avon)* **16**(6) (2001), 529–534.

**Reprinted from**

# Bio-Medical Materials and Engineering

(ISSN 0959-2989)

IOS Press

Amsterdam • Washington, DC • Tokyo

www.iospress.nl

# BIO-MEDICAL MATERIALS AND ENGINEERING
## AN INTERNATIONAL JOURNAL



**Aims and Scope**

The aim of *Bio-medical Materials and Engineering* is to promote the welfare of humans and to help them keep healthy. This International Journal is an interdisciplinary journal that will publish original research papers, review articles and brief notes on materials and engineering for biological and medical systems. Articles in this peer-reviewed journal will cover a wide range of topics, including, but not limited to: Engineering as applied to improving diagnosis, therapy, and prevention of disease and injury, and better substitutes for damaged or disabled human organs, such as drug delivery, medical devices, systems and artificial organs; Studies of biomaterial interactions with the human body, bio-compatibility, interfacial and interaction problems; Biomechanical behaviour under biological and/or medical conditions, such as, fracture toughness, fatigue, creep, stress corrosion cracking, corrosion fatigue, plasticity, visco-elasticity, rheology, tribology and wear, and behaviour under impact, mechanics and devices for promotion of physical strength; Mechanical and biological properties of membrane biomaterials; Cellular and tissue engineering, physiological, biophysical, biochemical bioengineering aspects; Implant failure fields and degradation of implants. Biomimetics engineering and materials including system analysis as supporter for aged people and as rehabilitation; Bioengineering and materials technology as applied to the decontamination against environmental problems; Biosensors, bioreactors, bioprocess instrumentation and control system; Application to food engineering; Standardization problems on biomaterials and related products; Assessment of reliability and safety of biomedical materials and man-machine systems; Product liability of biomaterials and related products.

**Publisher**
**IOS Press**
Nieuwe Hemweg 6B
1013 BG Amsterdam
The Netherlands

Tel.: +31 20 688 3355
Fax: +31 20 620 3419

E-mail:
Subscription Dept.: order@iospress.nl
Advertising Dept.: market@iospress.nl
Desk Editorial Dept.: editorial@iospress.nl

Internet:
www.iospress.nl